Tautomers of the N-centered radical generated by reaction of $SO_4^{\bullet -}$ with N1-substituted cytosines in aqueous solution. Calculation of isotropic hyperfine coupling constants by a density functional method

Sergej Naumov,[a] Knut Hildenbrand[b] and Clemens von Sonntag[b]

[a] *Institut für Oberflächenmodifizierung, Permoserstraße 15, D-04318 Leipzig, Germany*
[b] *Max-Planck-Institut für Strahlenchemie, Stiftstr. 34–36, PO Box 101365, D-45413 Mülheim an der Ruhr, Germany. E-mail: vonsonntag@mpi-muelheim.mpg.de; Fax: +49-208-306-3951*

Received (in Cambridge, UK) 20th February 2001, Accepted 5th April 2001
First published as an Advance Article on the web 4th May 2001

In the reaction of $SO_4^{\bullet -}$ with 1-methylcytosine, 2′-deoxycytidine (and with cytidine in the presence of HPO_4^{2-}) a very prominent radical is observed by EPR spectroscopy [*a*(N3), *a*(N4) 1.18, 1.16 mT; H. Niehaus and K. Hildenbrand, *J. Chem. Soc., Perkin Trans. 2*, 2000, 947], but its structure could not be assigned. In the present study, the isotropic hyperfine coupling constants (hfcs) of ten radicals that may be formed under such conditions were computed by a density functional method. Agreement between experimental and calculated couplings is achieved with the iminyl radical **4** [*a*(N3), *a*(N4) calculated 1.23, 1.17 mT]. This radical is formed upon deprotonation of the intermediate cytidyl radical cation **2** at the exocyclic amino group. The ensuing aminyl radical **3** then transforms into its tautomer **4** by migration of the proton from N4 to N3. This mechanism is supported by quantum-mechanical calculations of the energies of the radicals which show that the tautomerisation **3** ⟶ **4** is exothermic. The following alternative pathways have been discussed and the hfcs of the ensuing radicals have been calculated: (i) formation of OH-adduct radicals upon reaction of the cytidyl radical cation with water, (ii) disproportionation of the OH-adduct radicals and subsequent generation of oxyl radicals upon oxidation of a 5-hydroxycytosine derivative by peroxodisulfate, and (iii) recombination of the aminyl radicals and oxidation of the N–N-linked dimer with the formation of hydrazyl-type radicals. None of the calculated hfcs of the resulting radicals match the experimental values.

In the living cell, the DNA damage induced by ionising radiation has two components, the *direct effect*, where the energy of the ionising radiation is absorbed by DNA, and the *indirect effect*, where $^{\bullet}$OH radicals formed in the radiolysis of its aqueous environment damage the DNA.[1] The major event in the interaction of ionising radiation with DNA is the formation of base radical cations. For a better understanding of the ensuing processes, numerous experiments have been carried out on a model level in aqueous solution. In particular, the oxidation of pyrimidine derivatives by the sulfate anion radical $SO_4^{\bullet -}$ has been investigated in some detail with the help of stationary EPR spectroscopy.[2–9] The results obtained with uracil, thymine and their N1-substituted derivatives are explained by radical cations as intermediates which then undergo various reactions, *e.g.* deprotonation at N1 (uracil, thymine)[2,3] or at the C5-methyl group (thymidine-5′-phosphate),[4] transfer of the radical site to the ribose moiety (uridine, cytidine)[5–8] and formation of OH-adduct radicals by the reaction of H_2O at C5 or C6 (1-methyluracil, 2′-deoxyuridine, 1-methylthymine, thymidine).[4–9]

In contrast, a straightforward interpretation of the stationary EPR spectra generated by $SO_4^{\bullet -}$ with 1-methylcytosine **1a** and 2′-deoxycytidine (dC) **1b** was not possible. Pulse radiolysis experiments of the reaction of $SO_4^{\bullet -}$ with **1b** seemed to indicate the generation of the cytidyl radical cation **2b** [reaction (1)] and subsequent rapid deprotonation [reaction (2)] at the exocyclic amino group to yield the aminyl radical **3b** (Scheme 1).[10] This reaction sequence was corroborated by time-resolved EPR studies.[11]

In these experiments, radical cation **2a** was generated by electron transfer from 1-methylcytosine **1a** to the triplet state of

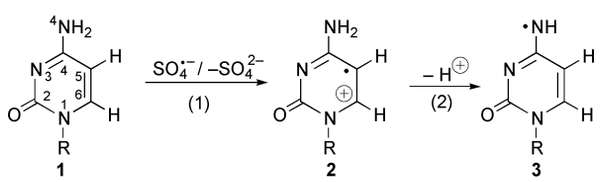

Scheme 1

anthraquinone-2,6-disulfonate, and the signals of radical **3a**, strongly enhanced by the CIDEP (chemically induced dynamic electron polarization) effect, were detected on the nanosecond time-scale. The spectrum of **3a** is characterised by a large doublet splitting of 1.74 mT due to the exocyclic NH proton which is replaced by a deuteron upon carrying out the reaction in D_2O instead of in H_2O [a(D) = a(H)/6.5 = 0.268 mT].

However, the stationary EPR spectra of cytosine derivatives[5,6,8] could not be explained by this simple model. Reaction of $SO_4^{\bullet -}$ with 1-methylcytosine and 2′-deoxycytidine[5,6] resulted in the spectra of a cytosine-derived radical (Fig. 1, **Xa,b**, simulated as **Xs**) consisting of five equidistant groups of signals with an intensity ratio of approximately 1 : 2 : 3 : 2 : 1.

In acidic solution, the spectra were very weak but increased in intensity at pH > 7 and in the presence of phosphate dianions.[5] The simulation in Fig. 1 (**Xs**) takes into account two large nitrogen splittings of 1.16 and 1.175 mT, a small nitrogen splitting of 0.18 mT and proton splittings of 0.11 (2 protons) and 0.09 mT. The small doublet of 0.09 mT collapsed when the experiments were carried out in D_2O. Because of the low signal

 DOI: 10.1039/b101680f

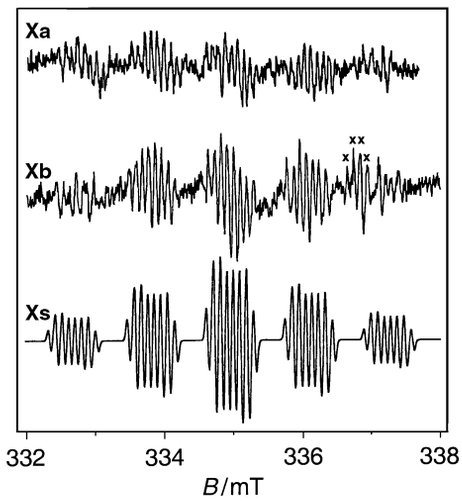

Fig. 1 Stationary EPR spectra obtained by the continuous-flow method upon UV-irradiation of aqueous solutions containing $K_2S_2O_8$, HPO_4^{2-} and 1-methylcytosine **1a** (**Xa**) or cytidine **1c** (**Xb**). Signals labelled with × are due to the acetonyl radical (in some experiments 1% acetone was added as photosensitiser; for details see refs. 5, 8). The simulated spectrum is denoted here and in the later figures as **Xs**.

to noise ratio and the contribution of polarised signals of the $^{\bullet}CH_2C(O)CH_3$ radical (*cf.* **Xb** in Fig. 1), agreement between experimental and simulated spectra was only moderate for the two signal groups at low and high field but good enough for the three groups in the central part of the spectrum to determine the hfcs with an error margin of <0.02 mT.

With cytidine, the situation was more complex due to the fact that the radical site generated in the primary step by reaction of $SO_4^{\bullet -}$ with the nucleobase is transferred from the radical cation **2c** to the ribose moiety [reactions (3) and (5)], and the resonances of the sugar radical **S** were detected (Scheme 2).[5–8]

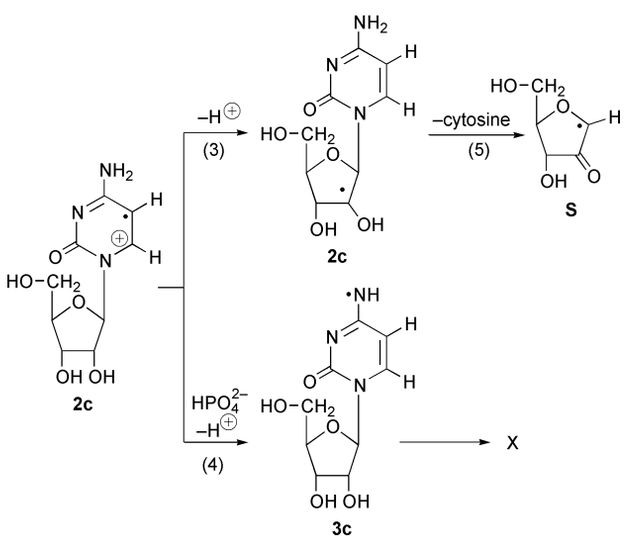

Scheme 2

However upon addition of phosphate (pH > 7.2), the spectrum of **S** decreased in intensity, and the spectrum of base radical **X** was observed instead[8] [reaction (4), see **Xb** in Fig. 1]. We have suggested that radicals **3** are formed by phosphate-catalysed deprotonation of the base radical cations **2** and rapidly transformed into **X**.[5,8] Hence, radicals **3** were not detected in stationary EPR experiments.

In order to support and to describe this assumption, we discuss in the following the relevant pathways which might be responsible for the formation of **X**. The hfcs of the radicals arising from these hypothetical reactions are calculated and compared with the experimental values with the goal to assign the structure of **X** and to shed some light on the reactions responsible for its generation.

Experimental

EPR experiments

The EPR experiments have been carried out on aqueous solutions containing the cytosine derivatives and $K_2S_2O_8$. Radicals were generated by UV-irradiation in a flow system and detected *in situ*.[5,8] The computer program[12] used for the simulation of the spectra is limited to eight interacting paramagnetic nuclei. Therefore, in some simulations small couplings were neglected (*cf.* Figs. 2 and 3).

Quantum chemical calculations

Density functional calculations of hyperfine coupling constants were carried out using the Hybrid B3LYP functional[13–15] in the Gaussian 98 program, revision A9.[16] The equilibrium geometries of the structures were optimised without restriction. The standard basis set 6-31G(d) was used, and the atomic charges as well as the atomic spin densities were calculated with the help of the Mulliken population analysis. To test the influence of water ($\varepsilon_r = 78$) on the molecular structure, the geometry was optimised with the help of the self-consistent reaction field (SCRF) Onsager (SCRF = dipole) model.[17] The effect of water on the spin density distributions and hfcs were also calculated using Tomasi's polarised continuum model (SCRF = PCM).[18,19]

Results and discussion

Some general remarks concerning the quantum-mechanical calculations

Density functional calculations proved to be a useful approach for the calculation of hfcs.[20] With pyrimidine-derived radicals, the geometry and the spin density distribution are strongly influenced by the solvent.[21] Solvent models on polarisable continuum dielectrics provide reliable solvent contributions. Tomasi's polarised continuum model (SCRF = PCM)[18,19] is a more realistic approach to mimic the solvent than the self-consistent reaction field (SCRF) Onsager (SCRF = dipole) model,[17] but it does not take into account possible changes of the molecular geometry. The influence of water on the geometry is especially important in the case of the OH-adduct radicals, where deviations from the planarity of the pyrimidine ring are significant. In water, the geometries were optimised by the SCRF = dipole method, and vacuum geometries were based on the SCRF = PCM method. The comparison of these geometries shows only a relatively small change of bond lengths and valence angles (maximal difference of 0.011 Å for interatomic distances and 0.8° for angles). However, considerable changes in the dihedral angles between α- and β-protons in the 5-yl and 6-yl radicals are observed (up to 4.2° for radical **7a**). The calculated spin density distributions and hfcs based on the SCRF = dipole and SCRF = PCM methods are qualitatively similar. However using the SCRF = dipole method, the average values of the hfcs are in slightly better agreement with experiment, and thus only these calculations are reported.

Potential routes to radical X

The half-life of the aminyl radical **3a** observed in time-resolved EPR measurements[11] on 1-methylcytosine was less than 2 μs which is too short to allow detection in steady-state EPR experiments, and instead of the expected resonances of **3a** a characteristic spectrum, consisting of five equidistant groups of signals, was observed (**Xa** in Fig. 1). A reaction which, in principle, may be responsible for the rapid disappearance of **3** and subsequent formation of **X** on the much longer time-scale of the stationary experiments is a tautomerisation [*cf.* reactions (6)

Table 1 Comparison of UB3LYP/6-31G(d) and Onsager SCRF = dipole models calculated hfcs (*a*/mT) with experimentally determined values for **Xs**, refs. 5 and 8

Position	Xs	3a[a]	4a	5a	6a(av)[b,c]	7a(av)[c]	8a(av)[c]	9a(av)[c]	14a	15a	17a[d]
N1	0.18	0.25 (0.20)	<0.01	0.04	0.14	0.04	0.14	0.09	0.32	0.31	0.12
N3	1.18	0.37 (0.43)	1.23	1.08	0.05	0.38	0.03	0.04	0.05	0.05	0.26
N4	1.16	1.08 (1.05)	1.17	1.20	0.07	0.06	0.04	0.68	0.05	0.10	0.87
H3	0.09		0.08				0.01	<0.01	0.01		
H5	0.11	0.35 (0.26)	0.18	0.15	2.43 (1.79)	1.98	1.99	0.90			0.16
H6	0.11	0.13 (0.14)	0.26	0.31	1.88 (1.79)	1.34	1.71	0.72	0.85	1.11	0.06
H, N4		1.77 (1.74)			0.05	0.08	0.04	1.04	0.09	0.15	
H′, N4					<0.01	0.11			0.10		
H, CH_3		0.39 (0.43)	0.03	0.04	0.25	0.01	0.24	0.28	0.38	0.39	
OH					0.42	0.19	0.31	<0.01			
Relative energy/ kJ mol^{-1}		0	−10.5	+54.0	0.0	−9.2	−8.4	−23.4	0.0	+17.6	

[a] Experimental values from ref. 11 in brackets. [b] Experimental values for 5-OH-6-yl radicals of cytidine and dC, ref. 7 in brackets. [c] Average values from Table 2. [d] *a*(N4′) 0.47, *a*(H, N4′) 0.79, *a*(N1′) 0.07, *a*(N3′) 0.13, *a*(H5′) 0.09, *a*(H6′) 0.02 mT.

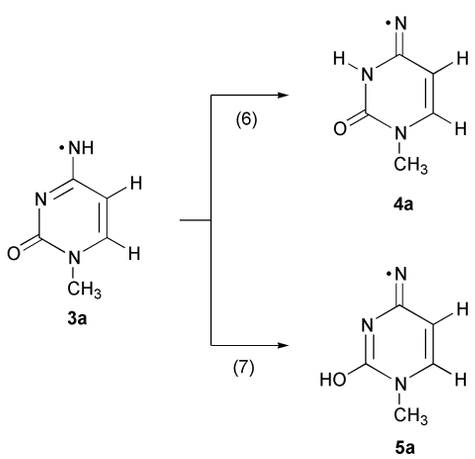

Scheme 3

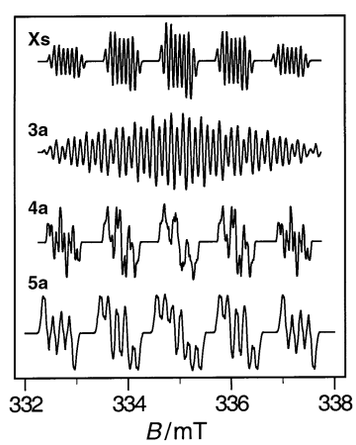

Fig. 2 EPR spectra simulated with the parameters given in Table 1 for radicals **Xs**, **3a**, **4a** and **5a**. For **3a**, *a*(H6) 0.15 mT was neglected, *cf*. experimental.

and (7)] (Scheme 3). On the other hand, the reaction of water at C5 or C6 of the intermediate radical cations is frequently observed upon the interaction of $SO_4^{\bullet -}$ with N1-substituted pyrimidines and therefore could also result in **X** [*cf*. reactions (8) and (9)] (Scheme 4). Moreover, the following secondary reactions might play a role: (i) generation of oxyl radicals upon oxidation of enolic products by $SO_4^{\bullet -}$ [*cf*. reactions (13)–(15)] (Scheme 6) and (ii) dimerisation and formation of hydrazyl radicals upon the subsequent oxidation of the dimer [*cf*. reactions (16) and (17)].

Tautomerisation of radical 3

Migration of the aminyl proton at N4 of **3** either to N3 [reaction (6)] or to O2 [reaction (7)] yields the iminyl radical **4** or **5** (Scheme 3). In Table 1, hyperfine couplings obtained by quantum-mechanical calculations on radicals derived from **1a** are compared with the experimentally determined hfcs of **X**.

With the data calculated for radicals **3a**, **4a** and **5a** (Table 1), the simulations in Fig. 2 have been generated.

Radicals **4a** and **5a** show two large nitrogen splittings, *a*(N3) and *a*(N4) (*cf*. Table 1). This explains the characteristic spectral pattern with five equidistant signal groups in close agreement with the results for **X**, whereas the parameters for **3a** are quite different. The small H couplings and an additional small nitrogen coupling are slightly different in experiment and calculation, and thus the internal splittings of the five individual groups do not fully match.

The assignment of **X** to the iminyl radicals **4a** or **5a** is supported by the fact that the *g* factor ($g = 2.0035$) and hfc *a*(N4) are in the range quoted for this type of radical[22–24] [*e.g.* for $CH_2{=}N^{\bullet}$: $g = 2.0031$ and *a*(N) 0.95–1.5 mT, depending on the solvent]. INDO calculations[25] on $CH_2{=}N^{\bullet}$ and our own calculations on **4** and **5** show that in these radicals most of the spin density resides in the p_y orbital of nitrogen, *i.e.* that it is in the plane, and that the nitrogen lone pair is in the 2s orbital.

Hence, it seems that deprotonation of the intermediate radical cation [*cf*. reactions (2) and (4)] and tautomerisation of the ensuing aminyl radical **3** [reactions (6) and/or (7)] can describe the formation of **X**. It is not possible, however, to predict merely on the basis of the coupling constants, whether structure **4a** or **5a** is responsible for the resulting EPR spectrum. Yet, the difference in the relative energies (based on **3** = 0: −10.5 kJ mol^{-1} for **4a** as compared to +54.0 kJ mol^{-1} for **5a**, see Table 1) strongly favours the N3-protonated tautomer **4a** generated in reaction (6). These calculations also show that the transformation **3a** ⟶ **4a** is exothermic, a prerequisite for this reaction to occur.

OH-Adduct radicals

The reaction of $SO_4^{\bullet -}$ with N1-methylated uracils yields the EPR spectra of OH-adduct radicals formed by reaction of water at C5 or C6 of the intermediate radical cations.[4–7,9] Thus, one could expect the formation of radicals **6** and/or **7** [reactions (8) and/or (9)] and possibly also their tautomeric forms **8** and **9** which result from a proton migration from the exocyclic amino group to N3 [reactions (10) and (11); proton migration to O2 is not energetically favourable] (Scheme 4).

Quantum-mechanical calculations on C5- or C6-centered radicals of pyrimidines are complicated by the fact that these species are not planar. Recently, it has been shown that 5,6-dihydro-6-thymyl and 5,6-dihydro-5-thymyl exist in two conformations.[26] Particularly for the 6-yl radical, the computed

Table 2 Comparison of the proton hfcs (a(H)/mT) and of dihedral angles φ/° calculated using the Onsager SCRF = dipole and Tomasi's SCRF = PCM models

		Conformer I		Conformer II		Average		
Structure	Parameter	Water PCM	Water dipole	Water PCM	Water dipole	PCM	dipole	Experiment
10	a(H5)/mT	0.20	0.20	4.24	4.09	2.22	2.15	1.83[b]
	a(H6)/mT	2.04	2.03	1.92	1.95	1.98	1.99	2.04
	φ/°	35.8	34.6	81.7	81.6			
	ΔE/kJ mol^{-1}[a]	0.0	0.0	−2.5	−5.0			
11	a(H5)/mT	0.42	0.35	4.42	4.36	2.42	2.35	1.83[c]
	a(H6)/mT	2.02	2.04	2.07	2.12	2.05	2.08	1.83
	φ/°	36.6	34.1	86.8	85.6			
	ΔE/kJ mol^{-1}	0.0	0.0	+3.8	+8.8			
6a	a(H5)/mT	0.79	0.75	4.54	4.11	2.72	2.43	1.79[d]
	a(H6)/mT	1.88	1.89	1.85	1.86	1.87	1.88	1.79
	φ/°	45.4	42.4	78.9	75.9			
	ΔE/kJ mol^{-1}	0.0	0.0	−11.7	−0.8			
7a	a(H5)/mT	1.96	1.99	2.00	1.95	1.98	1.98	
	a(H6)/mT	1.71	1.00	2.26	1.68	1.98	1.34	
	φ/°	49.7	47.3	55.8	51.6			
	ΔE/kJ mol^{-1}	0.0	0.0	+8.8	−1.7			
8a	a(H5)/mT	0.56	0.50	3.61	3.48	2.09	1.99	
	a(H6)/mT	1.93	1.89	1.53	1.53	1.73	1.71	
	φ/°	45.6	44.6	65.8	69.3			
	ΔE/kJ mol^{-1}	0.0	0.0	−16.7	−12.5			
9a	a(H5)/mT	1.92	1.91	1.91	1.88	1.92	1.90	
	a(H6)/mT	0.56	0.55	1.12	0.89	0.84	0.72	
	φ/°	39.8	40.5	44.5	43.7			
	ΔE/kJ mol^{-1}	0.0	0.0	−4.6	−2.1			

[a] ΔE/kJ mol^{-1}: energy difference between the two conformers. Experimental values are taken from [b] ref. 9; [c] ref. 27; [d] ref. 7 for cytidine and 2′-deoxycytidine.

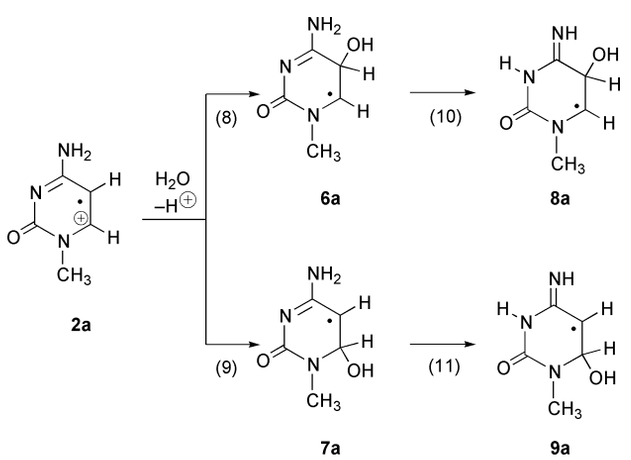

Scheme 4

β-H splittings of the conformers were widely different and vibrational averaging by the out-of-plane motion had to be taken into account to achieve agreement with the experimental data.

A similar situation is observed in our calculations on the OH-adduct radicals of pyrimidines. Because EPR data are not available for OH-adduct radicals of 1-methylcytosine, we first compared computed and experimentally determined α- and β-H couplings for the 5-OH-6-yl radicals **10** and **11** of 1-methyluracil[9] and of cytosine[27] (*cf.* Table 2). With the latter, the experimental EPR data were obtained in strongly acid solutions. For a comparison with experiment, we emphasise here our calculation of the protonated species, but our calculations

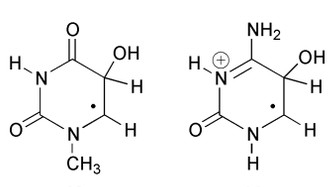

of the neutral species are very similar [a(H5) 0.82, 3.9 mT, a(av) 2.35 mT].

For both radicals, the calculations show two conformations with similar energies (*cf.* Table 2) but large differences in the dihedral angles φ(H5–C5–C6–H6) (**10**: 34.6 *vs.* 81.6°; **11**: 34.1 *vs.* 85.6°) and in θ, the dihedral angle of the unpaired electron with the C5–H5 bond (**10**, estimated: 8 *vs.* 55°; **11**: 4 *vs.* 56°). The axis of the orbital of the unpaired electron is approximately perpendicular to the C6–H6 bond, *i.e.* $\theta \approx 90° - \varphi$. However, since the spin density at C5/C6 is not exactly symmetrical, the $\cos^2$ θ-rule (*cf.* ref. 28) is only obeyed approximately.

The β-H splittings of conformers I are much smaller than those of conformers II (Table 2). Contrary to the calculations, in the experiments only a single set of couplings is observed. Hence, the two conformers I and II must undergo a rapid interconversion, and the observed hfcs thus represent the average a(av) due to a coalescence of the signals of the individual structures. When the average values are taken, a good agreement between calculations and experiment is obtained (*cf.* Table 2).

Wetmore *et al.*[29] have also calculated the hfcs of non-protonated **11**. They also obtain two conformers, but the differences in their β-proton splittings are significantly smaller [a(H5) 3.3 and 3.75 mT, a(av) 3.5 mT] than our values [a(H5) 0.82 and 3.9 mT, a(av) 2.35 mT], and their average value is not in line with the experimental value of 1.83 mT (Table 2). The reasons for these discrepancies are not known.

Energies and hfcs computed for the radicals **6**–**9** behave similarly. The α-H splittings are only slightly different for the two conformers. For the 6-yl radicals **6a** and **8a**, large variations are observed for the β-H splittings, with a very small value for conformer I and a very large one for conformer II.

We thus suggest that the average values should be close to the couplings expected from those radicals in solution. In fact, the values calculated for radical **6a** (derived from 1-methylcytosine) are in reasonable agreement with the hfcs reported for radicals **6b** and **6c** which were obtained by reaction of $^{\bullet}$OH with cytidine and 2′-deoxycytidine [reaction (12)] (Scheme 5).[7]

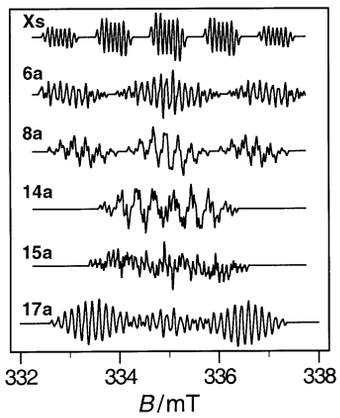

Fig. 3 EPR spectra simulated with the hfcs given in Table 1 for radicals **Xs**, the C5–OH-adduct radicals **6a** and **8a**, and for the secondary radicals **14a**, **15a** and **17a**. The following hfcs were neglected: **6a** *a*(N3) 0.05, *a*(H, N4) 0.05 mT; **8a** *a*(N3) 0.03, *a*(H, N4) 0.04 mT; **14a** *a*(N3) 0.05 mT; **17a** *a*(N1′) 0.07, *a*(H5′) 0.09, *a*(H6′) 0.02 mT and *a*(H6) 0.06 mT, *cf*. experimental.

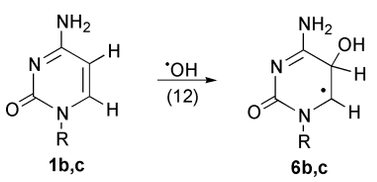

Scheme 5

For a comparison with **X**, the average couplings *a*(av) for radicals **6**–**9** are listed in Table 1. As examples, the characteristic spectra of the 6-yl radicals **6a** and **8a** with two large proton splittings are depicted in Fig. 3. Obviously, the parameters for the OH-adduct radicals are widely different from those of **X**, and a reaction of water at C5/C6 of the cytidyl radical cation cannot explain the formation of **X**.

Potential secondary reactions

Disproportionation of the OH-adduct radicals and subsequent formation of oxyl radicals. Reactions of $^{\bullet}OH$ and $SO_4^{\bullet -}$ with 4,6-dihydroxypyrimidines[3] and with N1-methylated uracils[9] yielded secondary radicals with a high spin density at oxygen. The formation of these radicals was explained by a rapid one-electron oxidation of reactive diamagnetic products originating from a disproportionation of C5–OH-adduct radicals. In a similar way, the oxyl radical **14a** and its tautomer **15a** may be generated from the OH-adduct radicals of the cytosine derivatives [reactions (13)–(15)] (Scheme 6).

However from the *g* factors ($g = 2.0035$ for **Xs**, $g \approx 2.0048$ for the secondary oxyl radicals derived from pyrimidines[3,9]) as well as from the hfcs, this pathway to **X** is excluded. Calculated hfcs for **14a** and **15a** are given in Table 1, and the corresponding simulated spectra are shown in Fig. 3. Contrary to the experimental data for **X**, the nitrogen couplings for **14a** and **15a** are small (<0.32 mT), and one of the proton splittings is large (0.85 mT for **14a** and 1.11 mT for **15a**).

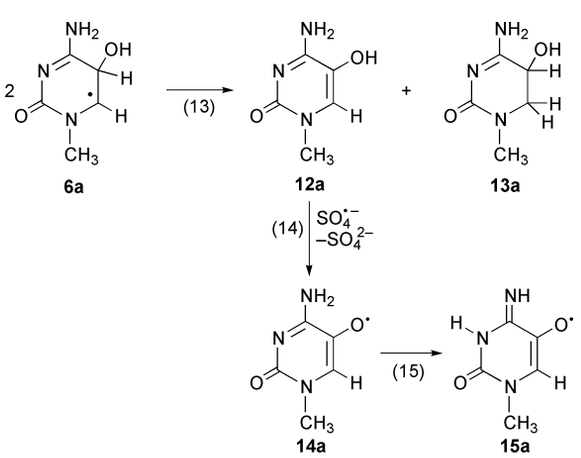

Scheme 6

Recombination of the aminyl radicals and subsequent oxidation of the resulting hydrazine derivative. In the absence of steric effects or of stabilisation by mesomeric effects, aminyl radicals tend to dimerise to hydrazine derivatives.[22] From the recombination of **3a** [reaction (16)] hydrazine derivative **16a** is expected to be formed. In a further oxidation step [reaction (17)] it could yield **17a** (Scheme 7).

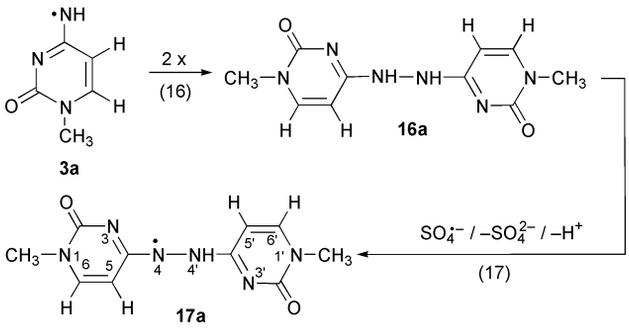

Scheme 7

From the comparison of hfcs calculated for **17a** (see Table 1 and Fig. 3) with those of **Xs**, it is obvious that this pathway has also to be excluded as an explanation of the spectrum obtained upon reaction of $SO_4^{\bullet -}$ with the title compounds.

Conclusions

Reaction of $SO_4^{\bullet -}$ with 1-methylcytosine, 2′-deoxycytidine (and with cytidine in the presence of HPO_4^{2-}) results in a characteristic stationary EPR spectrum consisting of five equidistant groups of signals with an approximate intensity ratio of 1 : 2 : 3 : 2 : 1. In order to assign the structure of the underlying species **X**, hfcs and relative energies for ten radicals which may possibly be generated under these conditions have been computed. Only the iminyl radical **4** with high spin density at N4 and N3 matches the requirements, *i.e.* two large nitrogen couplings of about 1.2 mT which give rise to the observed 1 : 2 : 3 : 2 : 1 pattern. The small H couplings and an additional small nitrogen coupling are slightly different in experiment and calculation, and thus the internal splittings of the five individual groups do not fully match. Radical **4** is formed upon deprotonation of the cytidyl radical cation **2** at N4 and subsequent transformation of the ensuing aminyl radical **3** into its tautomer **4** by a migration of the N4 proton to N3. Calculations of the relative energies of **3** and **4** have confirmed that the **3** ⟶ **4** transformation is exothermic.

References

1 C. von Sonntag, *The Chemical Basis of Radiation Biology*, Taylor and Francis, London, 1987.
2 K. M. Bansal and R. W. Fessenden, *Radiat. Res.*, 1978, **75**, 497.
3 H. M. Novais and S. Steenken, *J. Phys. Chem.*, 1987, **91**, 426.
4 K. Hildenbrand, *Z. Naturforsch.*, *Teil C*, 1990, **45**, 47.
5 K. Hildenbrand, G. Behrens, D. Schulte-Frohlinde and J. N. Herak, *J. Chem. Soc.*, *Perkin Trans. 2*, 1989, 283.
6 D. Schulte-Frohlinde and K. Hildenbrand, in *Free Radicals in Synthesis and Biology*, ed. F. Minisci, Kluwer, Dordrecht, 1989, p. 335.
7 H. Catterall, M. J. Davies and B. C. Gilbert, *J. Chem. Soc.*, *Perkin Trans. 2*, 1992, 1379.
8 H. Niehaus and K. Hildenbrand, *J. Chem. Soc.*, *Perkin Trans. 2*, 2000, 947.

9 G. Behrens, K. Hildenbrand, D. Schulte-Frohlinde and J. N. Herak, *J. Chem. Soc.*, *Perkin Trans. 2*, 1988, 305.
10 P. O'Neill and S. E. Davies, *Int. J. Radiat. Biol.*, 1987, **52**, 577.
11 J. Geimer, K. Hildenbrand, S. Naumov and D. Beckert, *Phys. Chem. Chem. Phys*, 2000, **2**, 4199.
12 F. Neese, Doctoral thesis, Computer Programme EPR, DOS version, University of Konstanz, 1993.
13 A. D. Becke, *J. Chem. Phys.*, 1993, **98**, 5648.
14 A. D. Becke, *J. Chem. Phys.*, 1996, **104**, 1040.
15 C. Lee, W. Yang and R. G. Parr, *Phys. Rev. B*, 1988, **37**, 785.
16 Gaussian 98, Revision A9, M. J. Frisch, G. W. Trucks, H. B. Schlegel, G. E. Scuseria, M. A. Robb, J. R. Cheeseman, V. G. Zakrzewski, J. A. Montgomery, Jr., R. E. Stratmann, J. C. Burant, S. Dapprich, J. M. Millam, A. D. Daniels, K. N. Kudin, M. C. Strain, O. Farkas, J. Tomasi, V. Barone, M. Cossi, R. Cammi, B. Mennucci, C. Pomelli, C. Adamo, S. Clifford, J. Ochterski, G. A. Petersson, P. Y. Ayala, Q. Cui, K. Morokuma, D. K. Malick, A. D. Rabuck, K. Raghavachari, J. B. Foresman, J. Cioslowski, J. V. Ortiz, A. G. Baboul, B. B. Stefanov, G. Liu, A. Liashenko, P. Piskorz, I. Komaromi, R. Gomperts, R. L. Martin, D. J. Fox, T. Keith, M. A. Al-Laham, C. Y. Peng, A. Nanayakkara, C. Gonzalez, M. Challacombe, P. M. W. Gill, B. Johnson, W. Chen, M. W. Wong, J. L. Andres, M. Head Gordon, E. S. Replogle and J. A. Pople, Gaussian, Inc., Pittsburgh, PA, 1998.
17 M. W. Wong, M. J. Frisch and K. B. Wiberg, *J. Am. Chem. Soc.*, 1991, **113**, 4776.
18 S. Miertus, E. Scrocco and J. Tomasi, *Chem. Phys.*, 1981, **55**, 117.
19 S. Miertus and J. Tomasi, *Chem. Phys.*, 1982, **65**, 239.
20 B. Engels, L. A. Eriksson and S. Lunell, *Adv. Quantum Chem.*, 1996, **27**, 297.
21 S. Naumov, A. Barthel, J. Reinhold, F. Dietz, J. Geimer and D. Beckert, *Phys. Chem. Chem. Phys.*, 2000, **2**, 4207.
22 W. C. Danen and F. A. Neugebauer, *Angew. Chem., Int. Ed. Engl.*, 1975, **14**, 783.
23 M. C. R. Symons, *Tetrahedron*, 1973, **29**, 615.
24 J. A. Brivati, K. D. J. Root, M. C. R. Symons and D. J. A. Tinling, *J. Chem. Soc. A*, 1969, 1942.
25 D. E. Wood, R. V. Lloyd and D. W. Pratt, *J. Am. Chem. Soc.*, 1970, **92**, 4115.
26 F. Jolibois, J. Cadet, A. Grand, R. Subra, N. Rega and V. Barone, *J. Am. Chem. Soc.*, 1998, **120**, 1864.
27 C. Nicolau, M. McMillan and R. O. C. Norman, *Biochim. Biophys. Acta*, 1969, **174**, 413.
28 R. O. C. Norman and B. C. Gilbert, *Adv. Phys. Org. Chem.*, 1967, **5**, 53.
29 S. D. Wetmore, F. Himo, R. J. Boyd and L. A. Eriksson, *J. Phys. Chem. B*, 1998, **102**, 7484.